Supporting Information

Mukherjee and Warshel 10.1073/pnas.1500979112

SI Text

General and Structural Considerations of the F₁-ATPase Rotary–Chemical Cycle. Despite the immense progress in understanding the overall F₁-ATPase functional cycle from structural, kinetics, and single-molecule experiments, a quantitative description of the structure–energy relationship behind the stepwise rotation of the motor is still needed. The primary challenge is to combine the biochemical and structural findings with a well-defined physical model that reproduces the observed directionality without modeling it through phenomenological parameters. To advance toward any kind of structure-based understanding of the torque generation process in F₁-ATPase, one must obtain a clear concept of the underlying free energy surface of the rotary–chemical process.

To study the rotary–chemical cycle that comprises the chemical and conformational/rotary events in the milliseconds range, it is essential (at least with the present computational capability) to adopt a reduced dimensionality approach so that we are able to formulate and answer questions relevant at the biological timescale. Thus, we start by using the available atomistic structure to model the large conformational changes with our CG model (1). The intermediates along the conformational/rotation coordinates have been already generated for our previous study on F₁-ATPase (2). Here, we depict the rotary intermediates for the central stalk for 240° rotation in Fig. S1. We also show in Fig. S2 the conformational transitions of the α/β-catalytic subunits from ADP bound form (D) to empty (E), empty (E) to ATP bound form (T), and ATP bound form (T) to ADP bound form (D). Using the conformational and rotational intermediates, we recalculate the conformational free energy landscapes, using our updated CG model (1), and show the maps for the wild type, the all-alanine γ-mutant, and the all-glycine γ-mutant in Fig. S3. Comparing our new map for the wild type (Fig. S3*A*) with the map obtained in figure 2A of ref. 2 shows that the stepwise rotary–chemical pathway is clearly maintained, although the relative barriers along the conformational path have reduced by 4–5 kcal compared with our previous map.

The CG Model Used to Generate the Electrostatic Free Energy Surface of the Conformational Transitions in F₁-ATPase. The present work uses a CG model that describes the main chains by an explicit all-atom model and represents the side chains as a simplified united atom model. This CG model provides a more advanced treatment of electrostatic effect than most current CG models. More specifically, the present model (1), which is a slightly modified version of our recent work (3), expresses the overall free energy as

$$\Delta G_{\text{total}} = \Delta G_{\text{main}} + \Delta G_{\text{main--side}} + \Delta G_{\text{side}}. \quad [\text{S1}]$$

The all-atom main chain is treated with implicit solvent corrections, and the main–side treatment involves van der Waals and screened electrostatic terms. The major and most relevant part of our treatment comes from the ΔG_{side}, which is given by

$$\Delta G_{\text{side}} = \Delta G_{\text{side}}^{\text{vdw}} + \Delta G_{\text{side}}^{\text{elec}} + \Delta G_{\text{hyd}}. \quad [\text{S2}]$$

The first term describes the effective van der Waals interactions between simplified side chains, which are described in ref. 3. The second term represents the electrostatic energy of the ionizable residues (see below) and the last term represents the hydrophobic contributions, which are not included implicitly in the first term.

The $\Delta G_{\text{side}}^{\text{elec}}$ term is given by

$$\Delta G_{\text{side}}^{\text{elec}} = -2.3RT \sum_i Q_i \left(pK_{a,i}^w - pH \right) + \Delta G_{QQ} + \Delta G_{\text{self}}, \quad [\text{S3}]$$

where i runs over the protein ionizable residues, $pK_{a,i}^w$ is the pK_a of the ith residue in water, and Q_i is the charge of the ith residue in the given ionization state. ΔG_{QQ} is the charge–charge interaction free energy, which is given by

$$\Delta G_{QQ} = \frac{\sum_i \sum_{j \neq i} 166 Q_i Q_j}{r_{ij} \varepsilon_{\text{eff}}}, \quad [\text{S4}]$$

where the energy is given in kilocalories per mole and the distances in angstroms. ε_{eff} is the effective dielectric for charge–charge interaction, which reflects the idea established in many of our works (e.g., refs. 3–5) that the optimal value is large even in protein interiors (namely $\varepsilon_{\text{eff}} > 20$). This type of dielectric has been found recently to provide very powerful insight in studies of protein stability (4, 5) and thus it is expected to be very useful in modeling the electrostatic contribution to the stability of the simplified model. The ionization states of the protein residues were determined by the Monte Carlo approach of ref. 3 for pH 7.0.

A key element in our approach is the treatment of the self-energy, ΔG_{self}, associated with charging each ionized group in its specific environment. This term is described in detail in ref. 3. Additional key features and more recent refinements of the treatment of the protein and the membrane system are described in the supporting information of ref. 6 and in ref. 1.

All of the above electrostatic modeling involves a self-consistent treatment of the interdependent self-energy, charge–charge interaction, and external pH (where the ionization state is determined by a Monte Carlo treatment of the energetics of Eq. **S3**).

Torque Calculations from the Rotary–Chemical Surface of F₁-ATPase. The electrostatic free energy maps of Fig. S3 have been used to calculate the torque generated for the wild-type and mutant F₁ systems. The map for single ATP hydrolysis and 120° rotation has been used to generate the rotary–chemical surface (Fig. 2 of main text). After generating the effective rotary–chemical surfaces (as shown in Fig. 2, *Upper Middle* and *Lower Middle*), the PMF is calculated using Eq. **2** (main text) along the rotational coordinate (shown in Fig. 2, *Bottom*). The free energy drop between the 0° and 120° rotational states is used to calculate the net average torque produced by the F₁ systems under study.

The stepwise feature of the conformational map in Fig. S3 *A* and *B* already shows that γ-rotation is tightly coupled to the α/β-catalytic subunit changes for the wild type and all-alanine γ-mutant. Thus, one way of adding the chemical free energy to the conformational surface was after γ has crossed the position of the "catalytic dwell" (that is, after 80°) and after α/β-catalytic subunits have completed half of the conformational changes starting from D₁E₂T₃ to E₁T₂D₃ (here E, T, and D represent the β-subunit in "empty," "ATP bound," and "ADP bound" forms and 1, 2, and 3 represent the catalytic subunit numbers). We also added the chemical free energy to all values of the rotational coordinate to further evaluate the effect on the torque generation. The free energy release after chemistry has been considered as 8 kcal/mol for cellular ligand concentrations. The electrostatic map for the all-glycine γ-mutant shows a very different trend where coupling between the γ- and α/β-subunits is completely destroyed. This implies that although the α/β-subunits could

possibly perform the chemical step and release the chemical free energy as implied in a recent experimental study performed on F_1-ATPase catalytic subunits without the central stalk (7), the same free energy release is not coupled to any specific angle of the γ-subunit during the rotary process. This also implies that the free energy release can now be effectively added to all values of the rotational coordinate giving rise to the trend observed in Fig. 2C of the main text.

Comparison with Other Studies of the Torque Generation. It seems to us that the unfamiliarity of some with the importance of using free energy landscapes in describing the action of complex biological systems (e.g., ref. 8) highlights the importance of clarifying the difference between our approaches and other current strategies of exploring the torque generation. In particular, we wish to clarify the problem with the implication that the targeted molecular dynamics (TMD) approach can reproduce the observed torque. Such an implication has been further emphasized in a recent work (9) that superimposed its experimental results and the simulated torque profile results of ref. 10, generating figure 5A of ref. 9). The relevant figure "compared" theoretical torque profile obtained from picosecond-TMD simulations of forced γ-rotation with experimental results in the milliseconds range. The seeming correspondence of the shapes of the two profiles led the authors of ref. 9 to the notion that the steric mechanism or van der Waals contacts are driving the rotary–chemical coupling in F1-ATPase (as implicated in ref. 10). However, what is missing from the above argument is the fact that the general shape of the theoretical torque profile is the trivial result of using a pulling force of $K (\gamma_\Phi - \gamma_{80°})^2$ to change one rotational state to the other. With this external force, the system starts with great acceleration and then starts to slow down when γ approaches 80°. In this case there is always a trend of pushing the peak toward the end point, giving a generic torque profile as in ref. 10. The fact that the calculations of ref. 10 do not correspond to the experimental results of ref. 9 is also highlighted from the torque profile that has been calculated from forced rotations of the γ-subunit. Moreover, this forced rotation is accomplished in less than 3 ns rather than modeling the biological action happening in the milliseconds range.

In discussing other possible traps associated with the use of TMD to understand the rotary–chemical process of F_1-ATPase,

we also mention the work of ref. 10 that reproduced the experimental observation of the stepwise rotary feature by using two structures, one with the γ-stalk around 0° and another with the γ-stalk slightly rotated by 20°–30°. The authors then used TMD to move between the two structures that obviously did show a substep around 85° from the starting structure. Also, note that the system could have been simulated with the opposite pair of structures, giving rotation in the opposite direction. We should clarify that this TMD approach will not lead to an understanding of the structure-based physical principles behind the experimentally observed catalytic dwell. To gain a physical insight of the rotation/dwell process, one must obtain the free energy landscape of the whole rotational process [as was done in our previous study (2)] and try to generate experimental observables from that surface. Thus, the inference of the study of ref. 10 and the support shown in the studies of refs. 9 and 11 about the steric or van der Waals-mediated unidirectional rotation and torque generation are not valid, to our best understanding. Our recent work highlights clearly that electrostatics do have a decisive role to play in shaping the rotary–chemical coupled surface of the F_1-ATPase system, even if all of the charged residues of the γ-subunit are mutated to alanine. This further highlights the importance of correctly modeling long-range electrostatic effects, considering proper pH-dependent terms mimicking the pK shifts arising due to environmental solvation effects (as done in our CG model of ref. 1).

Another important point overlooked by some works is the necessary condition of coupling the chemical free energy with the conformational changes, without which no torque could be generated at all. In the absence of any chemical energy modeled into the system, it is hard to envisage that the theoretical torque profile of ref. 10 could lead to any basic understanding of the unidirectional rotary–chemical process in the F_1-ATPase system. In fact, forcing the γ-subunit to rotate by TMD and then evaluating the resulting torque largely reflect the applied external TMD force and not the ATPase-generated force. Hence, it is hard to see how one can judge whether F_1 rotation is guided by van der Waals/steric or electrostatics or any other mechanism, using forced simulations or calculations based on models without proper chemical coupling.

1. Vicatos S, Rychkova A, Mukherjee S, Warshel A (2014) An effective coarse-grained model for biological simulations: Recent refinements and validations. *Proteins* 82(7): 1168–1185.
2. Mukherjee S, Warshel A (2011) Electrostatic origin of the mechanochemical rotary mechanism and the catalytic dwell of F1-ATPase. *Proc Natl Acad Sci USA* 108(51): 20550–20555.
3. Messer BM, et al. (2010) Multiscale simulations of protein landscapes: Using coarse-grained models as reference potentials to full explicit models. *Proteins* 78(5): 1212–1227.
4. Roca M, Messer B, Warshel A (2007) Electrostatic contributions to protein stability and folding energy. *FEBS Lett* 581(10):2065–2071.
5. Warshel A, Sharma PK, Kato M, Parson WW (2006) Modeling electrostatic effects in proteins. *Biochim Biophys Acta* 1764(11):1647–1676.

6. Dryga A, Chakrabarty S, Vicatos S, Warshel A (2012) Realistic simulation of the activation of voltage-gated ion channels. *Proc Natl Acad Sci USA* 109(9):3335–3340.
7. Uchihashi T, Iino R, Ando T, Noji H (2011) High-speed atomic force microscopy reveals rotary catalysis of rotorless F_1-ATPase. *Science* 333(6043):755–758.
8. Vilfan A (2014) Myosin directionality results from coupling between ATP hydrolysis, lever motion, and actin binding. *Proc Natl Acad Sci USA* 111(20):E2076.
9. Martin JL, Ishmukhametov R, Hornung T, Ahmad Z, Frasch WD (2014) Anatomy of F1-ATPase powered rotation. *Proc Natl Acad Sci USA* 111(10):3715–3720.
10. Pu J, Karplus M (2008) How subunit coupling produces the gamma-subunit rotary motion in F1-ATPase. *Proc Natl Acad Sci USA* 105(4):1192–1197.
11. Chiwata R, et al. (2014) None of the rotor residues of F1-ATPase are essential for torque generation. *Biophys J* 106(10):2166–2174.
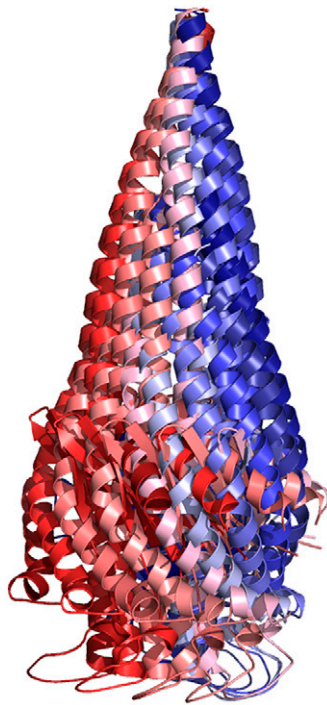
Fig. S1. Rotational intermediates for the γ-subunit shown for 240° rotations where the initial state (akin to PDB ID: 1H8E) is colored in deep red and the final 240° state is colored in deep blue with the intermediates colored in shades progressively passing from red to blue.
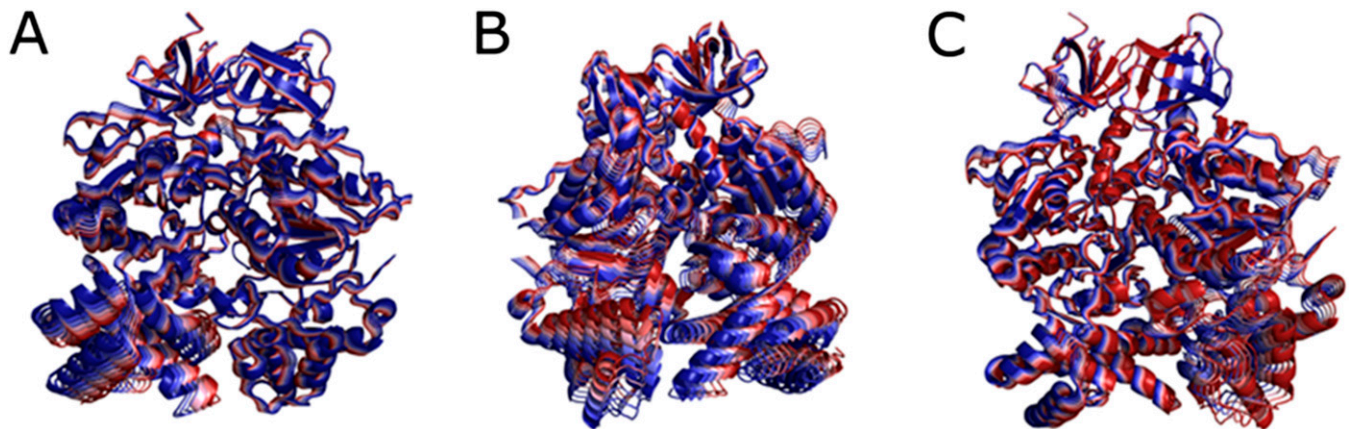
Fig. S2. Conformational intermediates for the α/β-subunits are shown for a single ATP hydrolysis cycle for (*A*) D_1 to E_1, (*B*) E_2 to T_2, and (*C*) T_3 to D_3. The coloring scheme is the same as in Fig. S1 where the state representing the crystal structure is colored in deep red with the intermediates colored in shades passing from red to blue.
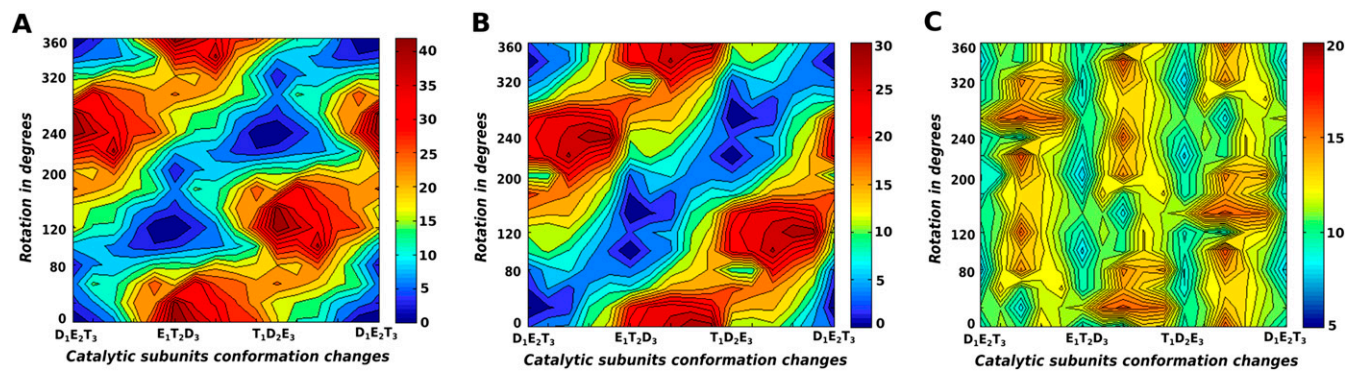
Fig. S3. Showing the CG electrostatic free energy surfaces, without the addition of chemical free energy, for 360° γ-rotation in the (*A*) WT system, (*B*) the all-alanine γ-system, and (*C*) the all-glycine γ-system.